AD-A034 901 COLORADO STATE UNIV FORT COLLINS HYDRO MACHINERY LAB F/G 20/4
POLYMER INJECTION INTO A DEVELOPING BOUNDARY LAYER.(U)
MAR 76 J P TULLIS, M POREH, J A HOOPER N00014-75-C-0274
UNCLASSIFIED HM-71 NL

| OF |

AD
A034901

END
DATE
FILMED
2-77

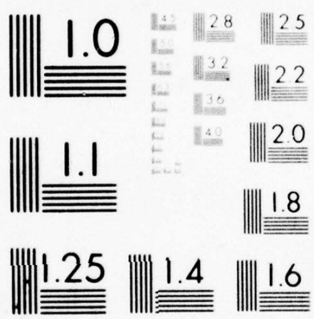
1.0
2.8
2.5
3.2
2.2
3.6
4.0
2.0
1.1
1.8
1.25
1.4
1.6

12

[illegible] INJECTION
INTO A [illegible] BOUNDARY LAYER

Final Report

by

[illegible]

and

[illegible]

[illegible]

[illegible]

POLYMER INJECTION
INTO A DEVELOPING BOUNDARY LAYER

Final Report

by

J. Paul Tullis
Michael Poreh

and

John A. Hooper

Engineering Research Center
Colorado State University
Fort Collins, Colorado

APPROVED FOR PUBLIC RELEASE: DISTRIBUTION UNLIMITED

This research was carried out under the
Naval Ship Systems Command
General Hydromechanics Research Program
Subproject SR 023 01 01, administered by the
Naval Ship Research and Development Center
Contract N00014-75-C-0274

March 1976

Hydro Machinery Laboratory
Report No. 71

TABLE OF CONTENTS

LIST OF FIGURES

LIST OF FIGURES (Cont'd.)

ABSTRACT

This report describes the last phase of a study on the drag reduction at the entrance region of a 12-inch pipe by injection of polymer solutions. In this phase of the study the effect of injecting concentrated solutions of WSR 301, up to 3600 ppmw, was examined.

This study indicates that the local friction downstream from the injector can be considerably reduced by increasing the discharge of the polymer injected into the pipe. However, the injection disturbs the flow and increases the pressure losses across the injector.

When the total drag reduction of a given pipe length (X/D), which includes the losses due to the injection, is considered, it is found that different optimal conditions exist for reducing the drag of short pipe sections and for reducing the drag of long pipe sections.

This report also summarizes a study of drag reduction in a pipe flow of Calgon TRO-375 solutions. For certain tests, this polymer caused an apparent increase in the effective roughness of the pipe walls. In addition, the report summarizes a study of the effect of a polymer (WSR 301) on the cavitation characteristics of a pipe orifice.

POLYMER INJECTION
INTO A DEVELOPING BOUNDARY LAYER

Chapter 1

INTRODUCTION

Unique facilities available at the Hydro Machinery Laboratory of the Engineering Research Center at Colorado State University made it possible to conduct an experimental study of drag reduction due to polymer injection into a developing boundary layer.

The purpose of the study has been to examine experimentally the effectiveness of various solutions of polymers as drag reducing additives, to examine the development of the boundary layer and the friction factors, to determine the dependence of the drag reduction on the concentration and the amount of the injected polymers, as well as to compare the efficiency of various injector designs.

The results of the earlier phases of the investigation have been documented in previous reports and publications (1,2,3,4,5). The purpose of this report is to report only the results of the last phase of the project in which the use of concentrated solutions (up to 3600 ppmw) was examined.

This report does not include our measurements of the concentration of the injected polymers along the developing boundary layer which have already been submitted to the sponsor. As evident from Table 1, almost 150 velocity profiles have been measured. No attempt has been made, however, to include in this report all the velocity measurements taken. At the end of this chapter we have included the original data for one run (Run 30) which consists of six figures drawn by the computer. The shape of the velocity profiles and the local friction reduction downstream of the injector are discussed in Chapter 2 of this report.

Chapter 3 of the report attempts to analyze the dependence of the total drag reduction of a given pipe length which includes the injector. The total drag reduction is a function of both the injection velocity and initial concentration. The analysis clearly indicates that the optimal conditions for increasing the total drag reduction differ for short systems and for long systems.

During this study parallel investigations of problems associated with the use of polymer solutions for drag reduction in different engineering applications were conducted at the Hydro Machinery Laboratory. Chapter 4 reports an observed phenomena of *effective roughness buildup* in solutions of Calgon TRO-375. Chapter 5 summarizes the results of an investigation on the effect of drag reducing polymers on the cavitation in an orifice flow and the degration of the polymers flowing through the orifice.

TABLE 1
List of Measured Velocity Profiles

Date	Run No.	Pipe Layout*	Water Flow (cfs)	Water Temp °C	Re x 10^{-5}	Polymer Injection Conc. ppm	C_∞ ppm	Injection Flow Rate gpm
June 26 1975	09	2	10.35	7.0	8.6	0	0	0
July 1975	10	2	5.59	8.0	4.8	0	0	0
July 1975	11	2	6.53	8.0	5.6	0	0	0
July 3 1975	12	2	22.36	9.0	19.77	0	0	0
July 3 1975	13	2	11.66	9.0	10.3	0	0	0
July 3 1975	14	2	16.75	9.0	14.8	0	0	0
July 8 1975	15	2	11.38	10	10.3	400	2.27	28.9
July 8 1975	16	2	8.963	10	8.15	400	20.2	202.9
July 9 1975	17	2	8.871	11	8.24	800	6.28	31.26
July 9 1975	18	2	8.778	11	8.16	800	12.0	55.0
July 9 1975	19	2	8.778	11	8.16	800	21.68	106.76
July 9 1975	20	2	8.778	11	8.16	800	33.7	166.2
July 11 1975	21	2	8.871	11	8.24	1600	12.4	30.75
July 11 1975	22	2	10.94	11	10.2	1600	12.2	37.4

*Velocity profiles were measured as follows: For pipe layout 1 at X/D = 5.8, 33.6 and 130.6. For pipe layout 2 at X/D = 11.5, 21.6 and 41.6. For pipe layout 3 at X/D = 17.9, 32.0 and 82.0. Positions of the manometers along the pipe are shown in the figures which show the layout filed with the data.

TABLE 1 (Cont'd.)

List of Measured Velocity Profiles

Date	Run No.	Pipe Layout*	Water Flow (cfs)	Water Temp °C	Re x 10^{-5}	Polymer Injection Conc. ppm	C_∞ ppm	Injection Flow Rate gpm
July 11 1975	23	2	22.72	11	2.1	1600	11.71	74.6
July 16 1975	24	2	10.66	9	9.4	Water	0	0
July 16 1975	25	2	10.7	9	9.5	400	3.3	40
July 16 1975	26	2	10.7	9	9.5	400	2.7	30
July 16 1975	27	2	10.73	9	9.5	400	6.7	80
July 16 1975	28	2	10.73	9	9.5	400	8.6	103
July 16 1975	29	2	10.73	9	9.5	400	4.77	57.4
July 17 1975	30	2	10.71	9	9.5	Water	0	0
July 17 1975	31	2	10.78	9	9.5	800	5.42	32.8
July 17 1975	32	2	10.76	9	9.5	800	7.79	47.0
July 17 1975	33	2	10.76	9	9.5	800	13.17	79.5
July 17 1975	34	2	10.76	9	9.5	800	21.7	131.
July 17 1975	35	2	10.76	9	9.5	800	27.0	163.
July 18 1975	36	2	10.69	9	9.5	Water	0	0
July 18 1975	37	2	10.76	9	9.5	1600	11.5	34.6
July 18 1975	38	2	10.76	9	9.5	1600	17.0	51.3
July 18 1975	39	2	10.76	9	9.5	1600	24.85	75.0
July 18 1975	40	2	10.76	9	9.5	1600	40.1	121.
July 18 1975	41	2	10.76	9	9.5	1600	54.3	164.
July 18 1975	42	2	10.76	9	9.4	1600	44.7	135.
July 22 1975	43a	2	10.68	9	9.5	Water	0	0
July 22 1975	43	2	10.74	9	9.5	3200	23.1	34.8
July 22 1975	44	2	10.74	9	9.5	3200	33.62	50.65
July 25 1975	45	3	10.69	9	9.5	0	0	0
July 25 1975	46	3	10.72	9	9.5	200	1.43	34.4
July 25 1975	47	3	10.72	9	9.5	200	2.49	60.0
July 25 1975	48	3	10.75	9	9.5	400	4.95	59.65
July 25 1975	49	3	10.75	9	9.5	400	6.82	82.3
July 25 1975	50	3	10.75	9	9.5	400	9.79	118.1
July 29 1975	51	3	10.80	8	9.2	1600	11.21	33.98
July 29 1975	52	3	10.80	8	9.2	1600	21.39	64.80
July 29 1975	53	3	10.82	8	9.2	1600	42.48	128.95
July 29 1975	54	3	10.81	8	9.2	1600	29.9	90.60
July 29 1975	55	3	10.85	8	9.3	3200	21.0	31.95
July 29 1975	56	3	10.85	8	9.3	3200	37.42	56.95

*Velocity profiles were measured as follows: For pipe layout 1 at X/D = 5.8, 33.6 and 130.6. For pipe layout 2 at X/D = 11.5, 21.6 and 41.6. For pipe layout 3 at X/D = 17.9, 32.0 and 82.0. Positions of the manometers along the pipe are shown in the figures which show the layout filed with the data.

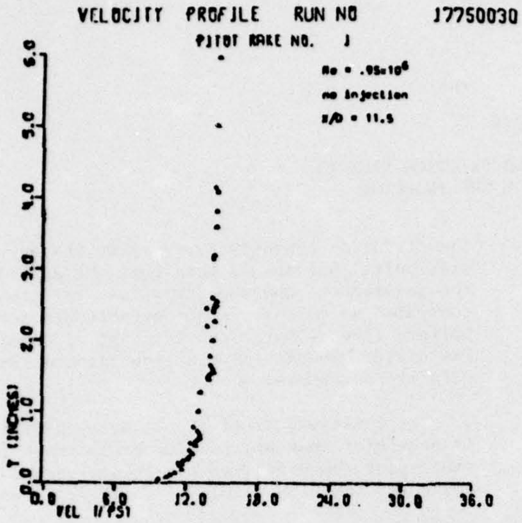
VELOCITY PROFILE RUN NO J7750030
PITOT RAKE NO. 1
Re = .95x10^6
no injection
X/D = 11.5
Y (INCHES)
VEL (FPS)

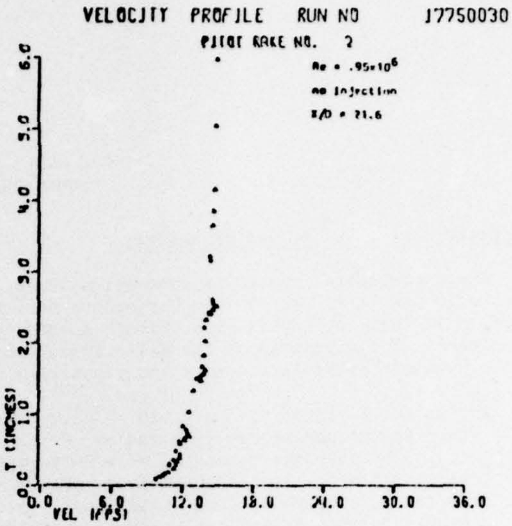
VELOCITY PROFILE RUN NO J7750030
PITOT RAKE NO. 2
Re = .95x10^6
no injection
X/D = 21.6
Y (INCHES)
VEL (FPS)

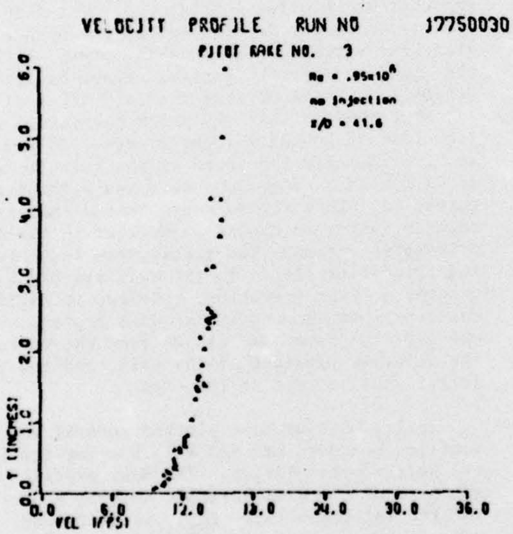
VELOCITY PROFILE RUN NO J7750030
PITOT RAKE NO. 3
Re = .95x10^6
no injection
X/D = 41.6
Y (INCHES)
VEL (FPS)

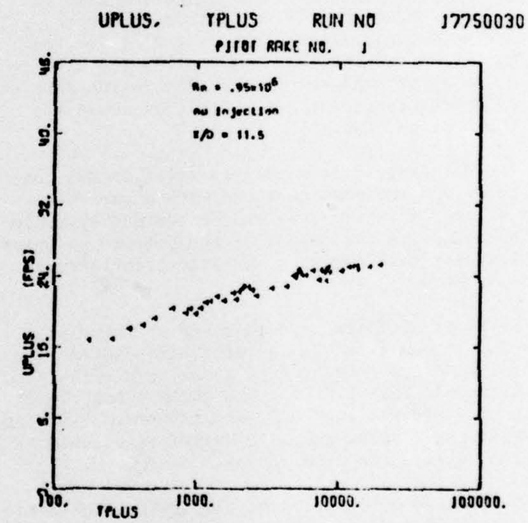
UPLUS, YPLUS RUN NO J7750030
PITOT RAKE NO. 1
Re = .95x10^6
no injection
X/D = 11.5
UPLUS (FPS)
YPLUS

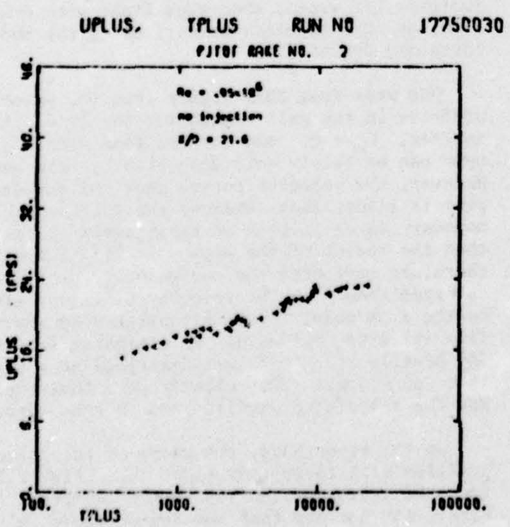
UPLUS, YPLUS RUN NO J7750030
PITOT RAKE NO. 2
Re = .95x10^6
no injection
X/D = 21.6
UPLUS (FPS)
YPLUS

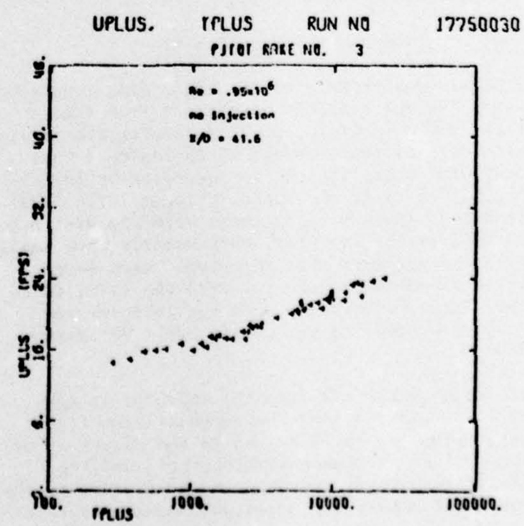
UPLUS, YPLUS RUN NO J7750030
PITOT RAKE NO. 3
Re = .95x10^6
no injection
X/D = 41.6
UPLUS (FPS)
YPLUS

Chapter 2

DRAG REDUCTION AND FRICTION FACTORS DOWNSTREAM FROM THE INJECTOR

The Experimental System and Procedure

The experimental system is schematically described in Fig. 2.1. Water from Horsetooth Reservoir enters a 12-inch horizontal pipe through a smooth transition. The discharge of the water is monitored by the pressure difference across the transition.

The injector was located at $X/D = 3.5$, where X is the distance downstream from the end of the transition. The injector consisted of a 2-ft length of a 12-inch diameter pipe in which four rows of 3/8-inch diameter holes were drilled at 30° angle to the pipe centerline. See Fig. 2.1(b). There were 48 holes per row providing a total injection area of 0.15 sq ft. The plenum of the injector was constructed with two 10-inch diameter 180° tube-turn fittings. The two fittings were welded together to form a "doughnut"-shaped plenum. The inside portion of this doughnut was cut out so that it would fit over the 12-inch pipe.

The discharge of the polymer solution was controlled by a Moyno pump equipped with a variable speed drive. The discharge was determined by measuring the change in the volume of the polymer solution in the supply tank during a measured time interval of steady flow.

Velocity profiles were measured at three stations downstream from the injector using three rakes of total head tubes. The tube sizes were 1/16-inch O.D. with 1/32-inch I.D. for the three tubes closer to the wall and 1/8-inch O.D. and 1/16-inch I.D. for the remaining five tubes. The entire rake could be traversed across the pipe radius.

A detailed description of the system, the data logging system and the experimental procedure is given in previous reports (2,5).

Friction Reduction and Velocity Profiles

Typical measurements of the local drag reduction (LDR) at different stations downstream from the injector are shown in Fig. 2.2. The results are consistent with earlier measurements which indicate that the local drag reduction can be increased by injecting more polymer into the boundary layer. The local drag reduction appears to decrease with the distance downstream from the injector, particularly when small quantities of polymers were injected. When large quantities of polymers were injected the local friction immediately downstream from the injector was drastically reduced and values of LDR > 90% were recorded.

The flow downstream from the injector is nonuniform. The velocity and the concentration fields vary both normal to the flow and in the direction of the flow. Since the concentration field and the velocity field are not independent, prediction of the development of either the momentum boundary layer or the diffusion boundary layer is at the very best difficult. One should note that the dependence of the friction on the concentration, for highly concentrated solutions, is not established even for uniform flows. Moreover, the initial conditions immediately downstream from the injector in our case are not known.

The measurements of the velocity profile make it possible, however, to deduce important information about the effect of the injection and the cause for the high values of local drag reduction.

Typical velocity profiles downstream from the injector are plotted in Fig. 2.3. The figure clearly shows the development of the boundary layer along the entrance region of the pipe. Although δ, the boundary layer thickness, cannot be accurately determined, it is obvious that at $X/D = 21.6$, δ is still smaller than R which suggests a rather slow rate of boundary layer growth. In Fig. 2.4, we have compared the shape of the velocity profile at $X/D = 11.5$ for flows with and without polymer injection. This figure suggests too that the boundary layer thickness is smaller in the flow with polymer injection. The figure also indicates that the velocities closer to the wall are higher in the case of polymer injection, however, it fails to describe what happens in the wall region. In fact, one gets the wrong impression from the curves that the velocity gradient at the wall, and the shear, is larger when polymer is injected.

In Fig. 2.5 we have plotted several velocity profiles measured at $X/D = 11.5$ using the law of the wall representation. The four profiles were measured at the same Reynolds number, 0.95×10^6, but the injection rate (C_∞) is different. On the same figure we have also plotted several velocity profiles for established pipe flows with drag reduction, at this Reynolds number, using the model of Poreh and Dimant (7).

One sees from this figure that the velocity profiles in the wall region for the flow without polymer, $C_\infty = 0$, and for the flow with $C_\infty = 5.4$ ppmw can be fairly well described by this model. However, the velocity curves near the center of the pipe is almost flat, because the thickness of the boundary layer in each of these cases is smaller than the radius of the pipe. In Fig. 2.6 we have therefore replotted the two velocity profiles and compared them with the velocity profiles calculated by the same model for an established boundary layer flow using the values of δ estimated from the data. The profile at $y > \delta$ was described by a straight line $u^+ = \text{const}$. One clearly sees that the measured and the calculated profiles are in good agreement.

On the other hand, the shape of the velocity profiles with larger values of C_∞, Fig. 2.5, differ from the calculated curves in two important features. First, one notices that the region where $u^+ = \text{const}$

has shrinked. In fact, it appears that there is a velocity gradient almost up to the center of the pipe, indicating a larger thickness of the boundary layer. Second, one sees that the velocities near the wall are smaller than the calculated velocities for an established boundary layer flow with the same friction reduction.

The same pattern was observed in almost all the experiments. When the amount of polymer injected was small, intermediate values of local drag reduction were obtained. The thickness of the boundary layer at $X/D = 11.5$ was small and the velocity profiles within the boundary layer resembled those recorded in established flows.

When C_∞ was large, the shear at $X/D = 11.5$ was further decreased but the thickness of the boundary layer there increased and the velocities closer to the wall did not follow the shape of the corresponding profile curves measured in established flows.

There seems to be a contradiction between the observation of a largely reduced shear and a faster development of the boundary layer. A reduction of the shear will usually attenuate the rate of growth of the boundary layer. Why then was the value of δ decreased when a small quantity of polymer was injected, but it increased when the injection rate became large? It seems that the injection of a large quantity of polymer has disturbed the flow near the injector. The disturbance caused a larger growth and as we shall see later a large pressure loss across the injector. Downstream from a disturbance a smaller shear is usually observed and the velocities very close to the wall are reduced, as found in this case.

Since the shear at the wall is small and the normal transport of momentum is largely reduced by the polymer, the flow downstream adjusts itself at a rather slow rate. In Fig. 2.7 velocity profiles were plotted at three stations downstream from the injector, for a typical flow with an intermediate injection rate of polymer. As can be seen from this figure, the boundary layer develops at a rather slow rate and the velocity profiles at each section are similar to those measured in established flows. Note that the length of the horizontal line at the outer region of each profile, where $u^+ = \text{const}$, is proportional to $1 - \delta/R$. In Fig. 2.8 velocity profiles were plotted in a typical case of large rate of polymer injection. The effect of the injection has been to increase the boundary layer thickness at $X/D = 11.5$ and change the shape of the velocity profile there. The boundary layer will eventually adjust but this process is slow, particularly when C_∞ is very large, and the effect of the disturbance is recognized even at $X/D = 41.6$.

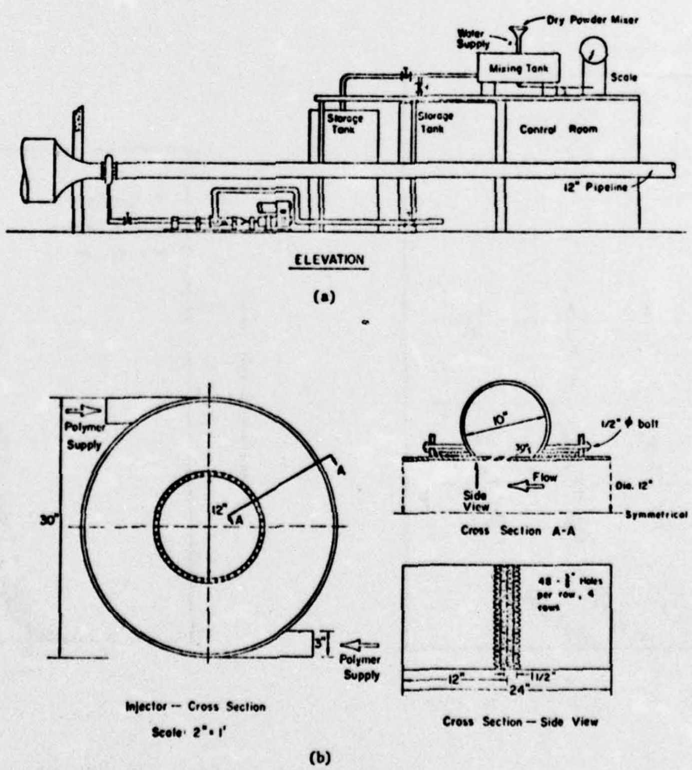

Fig. 2.1 The experimental system

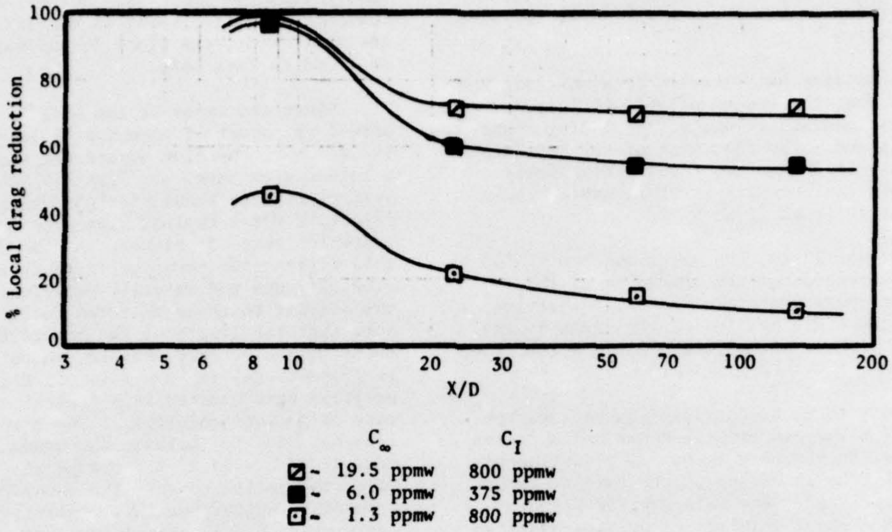

Fig. 2.2 Local drag reduction vs. X/D

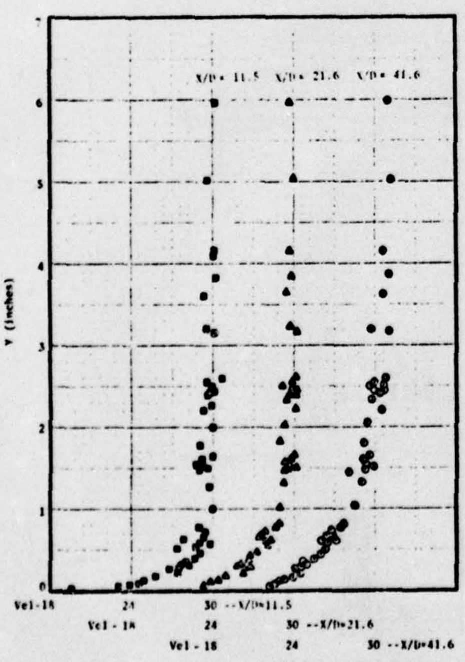

Fig. 2.3 Velocity profiles for three locations with WSR-301, 11.7 ppmw

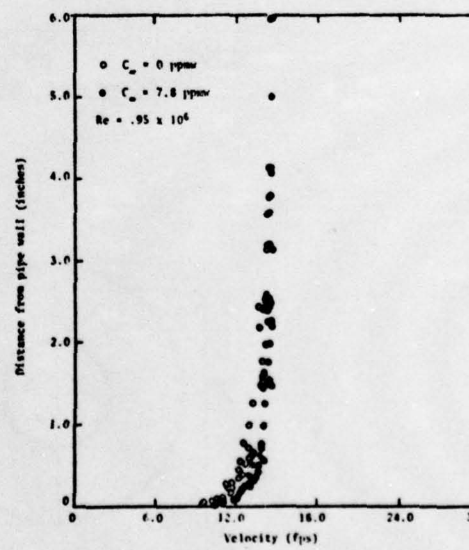

Fig. 2.4 Velocity profiles at X/D = 11.5 with and without polymer injection

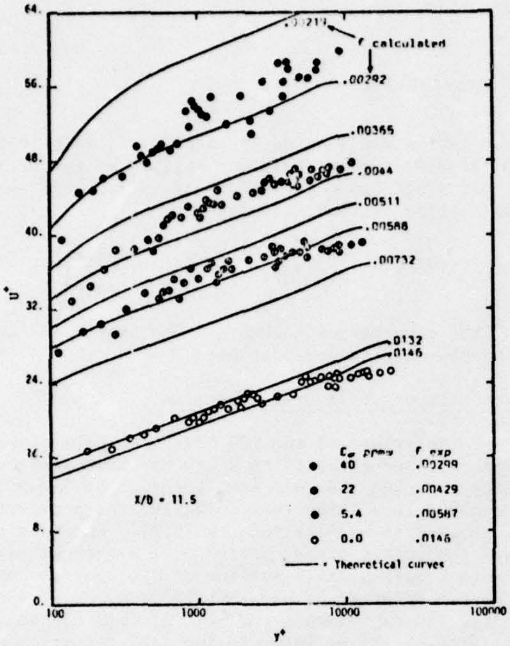

Fig. 2.5 Velocity profiles at X/D = 11.5 for different C_∞

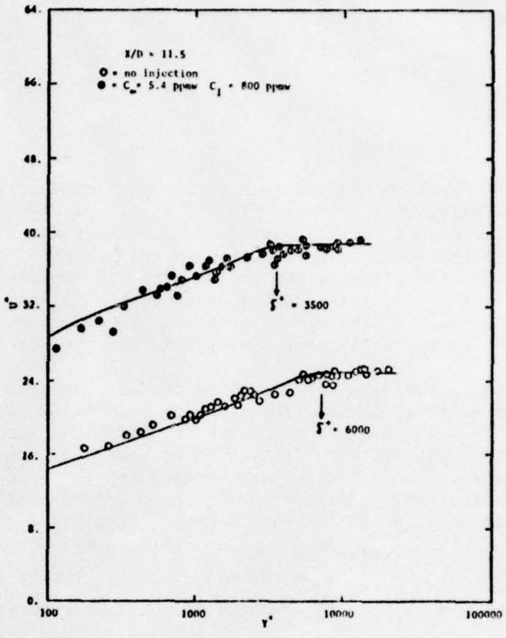

Fig. 2.6 Velocity profiles for zero and small C_∞

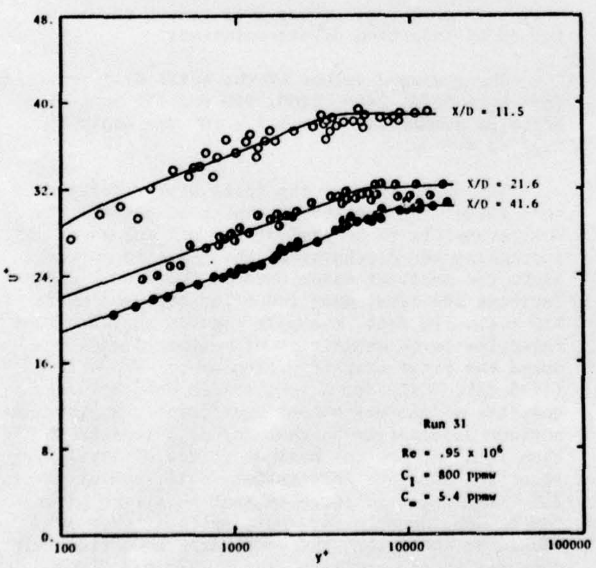

Fig. 2.7 Development of the velocity profiles, C_∞ = 5.4 ppmw

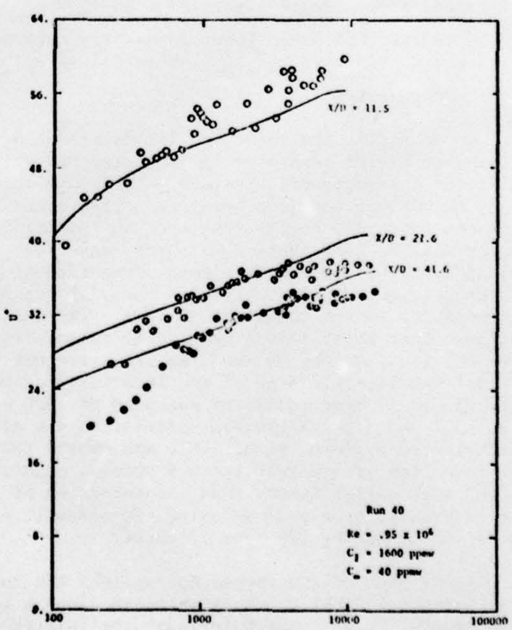

Fig. 2.8 Development of the velocity profiles, C_∞ = 40 ppmw

Chapter 3

TOTAL DRAG REDUCTION WITH WSR-301

Injection Losses

Previous studies (2,6,8) in pipes have already indicated that the injection of concentrated polymer solutions at the wall causes local losses which reduce the total drag reduction in the system. These losses are probably due to the disturbance created by the jet of the injected concentrated polymer solution and the high viscosity which that solution renders to the wall layer downstream from the injector.

To evaluate the injection losses, the head loss was measured between the stations $X/D = 1.5$ and $X/D = 5.75$ and compared with the head loss across this section without injection at the same Reynolds number. (The injector was located at $X/D = 3.5$.) The increase in percent of the head loss, namely the drag increase across the injector, is plotted versus the ratio $V_{water}/V_{injector}$ in Fig. 3.1. The velocity V_{water} denotes the average velocity in the pipe and $V_{injector}$ denotes the average velocity of the injected solution. The data clearly indicates that the losses across the injector are determined primarily by the injection velocity. Note that in these experiments the shear velocity V^* (upstream from the injector) was approximately constant and of the order of $V_{water}/25$. Thus it appears that the injection losses became significant when $V_{injector}/V^*$ is larger than one. Lower losses are obtained for a given $V_{water}/V_{injector}$, when dilute solutions are injected.

Undoubtedly, the injection losses are also determined by the design of the injector and primarily by the angle of injection. Therefore, one tends to measure the local drag reduction downstream from the injector, hoping that when an optimal injector will be used those local drag reduction values would be close to the total drag reduction of the system. However, it seems that, at present, the injector losses cannot be ignored. The data indicate that these losses seem to be correlated with the local values of the drag reduction not only in the immediate vicinity of the injector, but even with the local drag reduction measured at $X/D = 80$, Figs. 3.2 and 3.3. A similar correlation was also demonstrated by Poreh et al. (6), who showed that the injection of a purely viscous sucrose solution caused far smaller losses than the injection of the same discharge of a drag-reducing viscoelastic polymer solution having the same viscosity.

It is thus of importance to consider the Total Drag Reduction (TDR) which is obtained along a given pipe length (X/D), which includes the injector, and determines its dependence on both the injection concentration (C_I), the discharge of the polymers q and the injector geometry. Note that q is proportional to the "homogeneous concentration" C_∞ obtained far downstream when the concentration in the pipe becomes homogeneous. Since the injector in our system was located at $X/D = 3.5$, we have defined total drag reduction at any station as the drag reduction between the station $X/D = 1.5$ and that particular station, namely,

$$TDR(X/D) = 1 - \frac{[H(1.5) - H(X/D)]_{polymer}}{[H(1.5) - H(X/D)]_{water}}$$

at the same Reynolds number. The symbol H denotes the piezometric pressure head.

Analysis of Total Drag Reduction

The values of the TDR have been determined in a series of experiments in which the same master solution was used. A 3636 ppmw solution of WSR 301 was prepared in a large tank following the procedure described in earlier reports (2,5). The solution was thoroughly mixed, stored over night and mixed again. Only a small portion of the tank was used in the first series of experiments with $C_I = 3636$ ppmw. After the experiments the rest of the solution was diluted by adding water to the tank and stirring. The same procedure was used over until C_I decreased to 375 ppmw. It is quite possible that the repeated dilution and stirring caused some degradation. It does not seem to the authors that this degradation was significant but at least this procedure eliminated the possibility that the diluted polymer solutions were of a better quality than the more concentrated ones. This point is stressed because, as will be seen later, better drag reduction was obtained by injecting dilute solutions.

The measured values of the total drag reduction for $C_I = 3636$, 2466, 1200, 800 and 375 ppmw at a Reynolds number of $Re = 1.5 \times 10^6$ are shown in Figs. 3.4-3.8.

The dependence of the total drag reduction up to a given X/D on the discharge of polymer injected appears to be similar for all values of C_I. Increasing the discharge of the injected polymer, above the smallest value used in the study, did not increase the total drag reduction measured up to $X/D = 15$. In fact, the data clearly indicate that injecting large quantities of polymer always reduced the total drag reduction up to $X/D = 11.5$ (11.5 ft). Only for a long system does a larger quantity of polymer become beneficial. Another important observation is that for pipe lengths smaller than 15 diameters the maximum values of total drag reduction obtained were rather small, approximately 20%. This clearly suggests that this type of injector is not adequate for short systems. Now it should be noted that the local drag reduction values measured in the section between $X/D = 5.75$ and $X/D = 20$ were rather high as shown in Figs. 3.7 and 3.8. In fact, higher local drag reduction values correspond to lower total drag reduction values for this length. The maximum total drag reduction up to $X/D = 15$, for instance, was obtained with a very small amount of polymer ($C_\infty = 0.45$ ppmw) (see Fig. 3.8). An increase of 12 times in the amount of

polymer (C_∞ = 6 ppmw) caused such losses at the injector that the additional reduction of the local friction downstream could offset these losses only beyond X/D = 12.

The very large values of the measured local drag reduction at X/D = 8.5, which approached in some cases the 100% value, seem to be questionable at first. The same phenomena was recorded earlier in a 2-inch pipe (6). One could argue that the manometers in this region are effected by the concentrated solution. This argument if not supported, however, by the observation that these high values occurred primarily in the less concentrated solutions whenever the discharge of the injected solution was high. It is more plausible that the disturbance of the injected polymer created an effect similar to a venturi or an orifice effect. Namely, the velocities near the wall downstream from the disturbance are drastically reduced, whereas, the velocities closer to the core of the pipe are increased. This observation is consistent with the measurements of the velocity profiles reported in Chapter 2, but unfortunately these profiles were not measured closer than 8 diameters to the injector. This disturbance reduces the shear and the pressure gradient downstream, but the total drag across the disturbance is of course increased. In fact, if the disturbance is very large, the direction of the shear and pressure gradients immediately downstream from the injector can be reversed (pressure recovery downstream of an orifice throat). Such negative pressure gradients downstream from an injector had been reported earlier (6) and were also observed in this study. It should be stressed that the same phenomena can occur in external boundary layer flows. In such flows, a disturbance near the wall increases the growth of the boundary layer and the total drag, but, the local shear downstream from the disturbance is reduced. For this reason, the separation between the injector losses and the local drag reduction is not fully justified.

The results presented so far clearly indicate that the optimal injection concentration depends on whether one is interested in reducing the drag of a short system or a long system. Different optimal values will have to be chosen for a short boundary layer (L ~ 15 ft) and for a long boundary layer.

The effect of the injection concentration on the total drag reduction for a given discharge of polymer at the same Reynolds number (C_∞) is demonstrated in Figs. 3.9-3.13. In each of these figures, the data with a given C_∞ is plotted versus X/D with C_I as a variable. One sees that when C_∞ is large, injected solutions with higher values of C_I are more effective, probably due to lower injected velocities. However, the trend is changed when C_∞ is reduced below 8.5 ppmw (Fig. 3.11). These figures do not clearly demonstrate, however, the dependence of the drag reduction on C_∞ which appears to be more significant.

In Figs. 3.14-3.17, the total drag reduction up to X/D = 181.4, 81.7, 33.5 and 11.5 are plotted as a function of C_∞. It should be recalled that one would like to minimize the value of C_∞ in order to decrease the amount of polymer required. The data for X/D = 181.4, in Fig. 3.14, clearly indicates that the total drag reduction in a long pipe, or a long boundary layer increases with C_∞. A slightly higher drag reduction is obtained by injecting dilute solutions but this gain is not substantial and in view of the technical difficulties involved, it appears that a high or an intermediate value of C_I would be the optimal one.

The total drag reduction up to X/D = 81.7 (Fig. 3.15) also increases with C_∞ but the slope $d(TDR)/d(C_\infty)$ becomes smaller. When the total drag reduction of the pipe up to X/D = 33.5 is analyzed (Fig. 3.16), one finds that it does not increase any more with C_∞, beyond C_∞ of the order of 10 ppmw.

The dependence of the total drag reduction of a short pipe up to X/D = 11.5, is however, reversed. Figure 3.17 clearly indicates that higher values of total drag reduction are obtained with smaller quantities of polymer by injecting dilute concentrations.

It is interesting to note in this figure that when large quantities of polymer are used, say C_∞ = 10, better results are obtained with higher values of C_I, which corresponds to smaller values of $V_{injection}$. This indicates that the injection velocity is the primary cause for the losses at the injector, and that the effect of the injection concentration is secondary.

The results obtained are consistent with those obtained by Poreh et al. (6) in a 2-inch pipe. Both studies clearly indicate that for short systems, better drag reduction is obtained by reducing the concentration of the injected solution. In doing so, the total amount of polymer can be drastically reduced. Unfortunately, the maximum total drag reduction which can be obtained in a short system with this type of injector is not very large.

In the case of long systems, the significance of the injection losses is reduced and the total drag is primarily a function of the amount of the polymer injected into the flow, namely, C_∞.

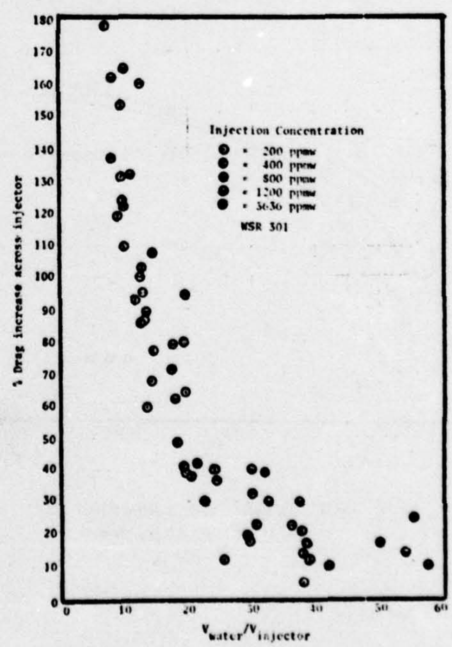

Fig. 3.1 Drag increase across the injector

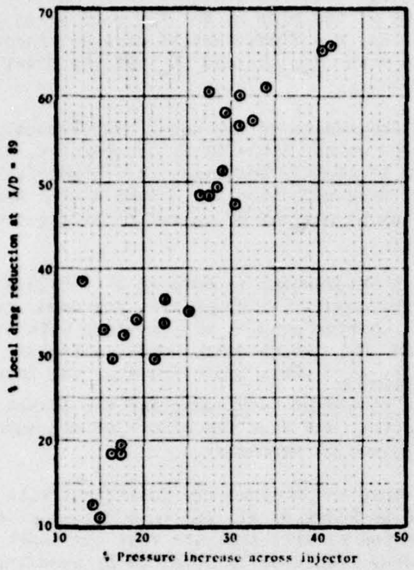

Fig. 3.2 Local drag reduction at X/D = 89 vs. pressure increase across injector (data from ref. 1)

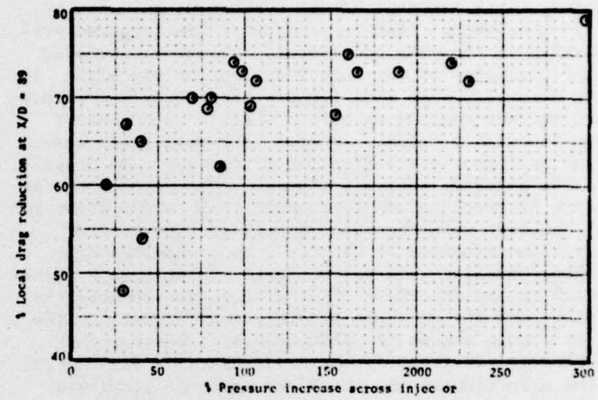

Fig. 3.3 Local drag reduction at X/D = 89 vs. pressure increase across injector (data from ref. 1)

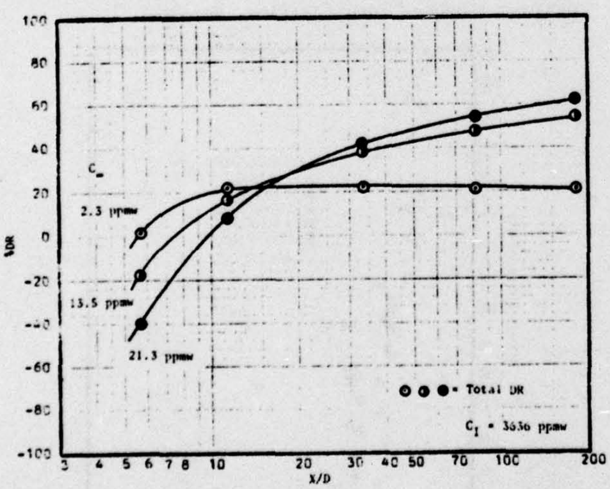

Fig. 3.4 Total drag reduction vs. X/D (C_I = 3636 ppmw)

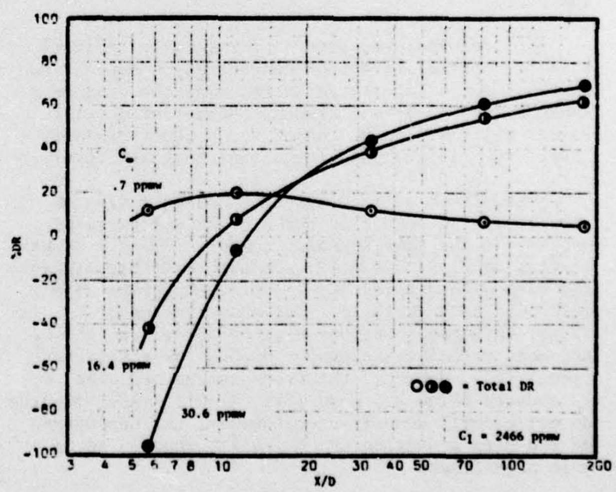

Fig. 3.5 Total drag reduction vs. X/D (C_I = 2466 ppmw)

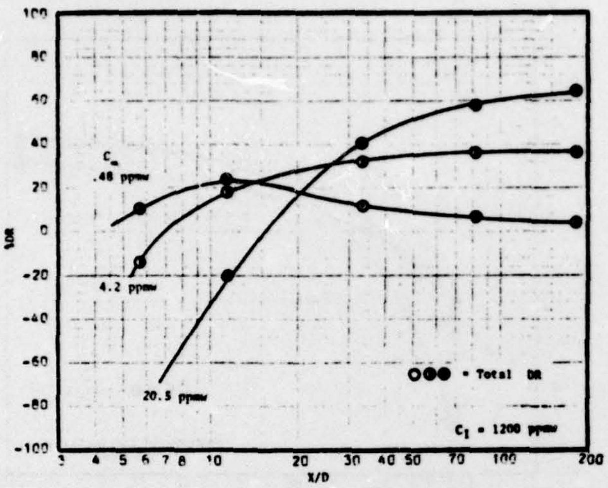

Fig. 3.6 Total drag reduction vs. X/D (C_I = 1200 ppmw)

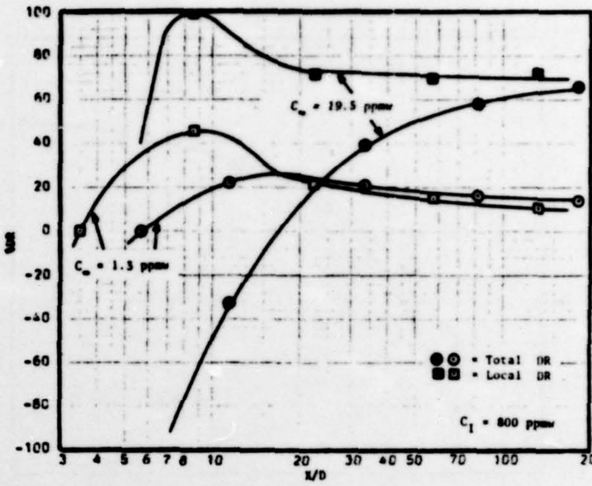

Fig. 3.7 Drag reduction vs. X/D (C_I = 800 ppmw)

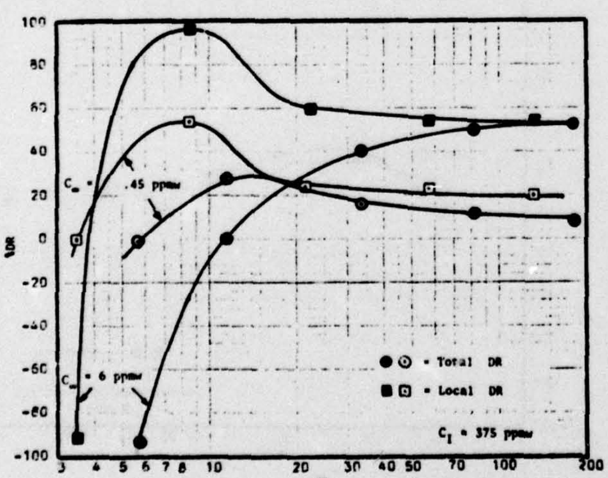

Fig. 3.8 Drag reduction vs. X/D (C_I = 375 ppmw)

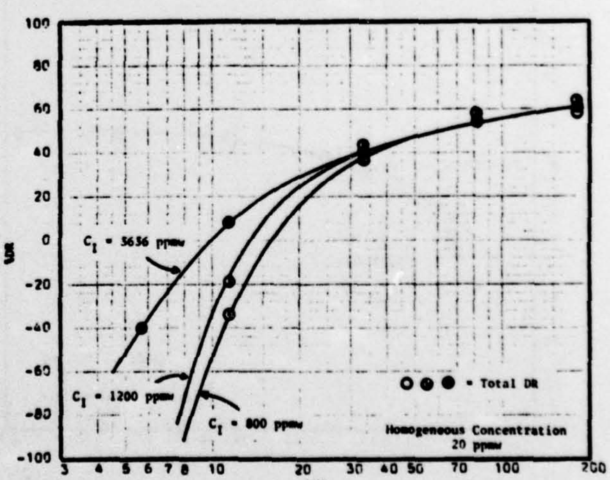

Fig. 3.9 Total drag reduction vs. X/D (C_∞ = 20 ppmw)

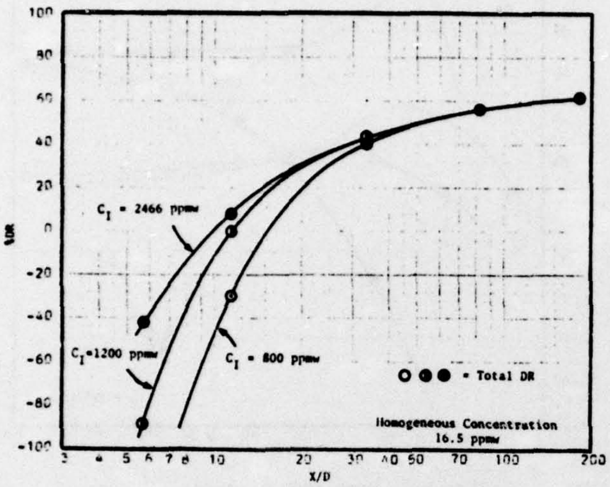

Fig. 3.10 Total drag reduction vs. X/D (C_∞ = 16.5 ppmw)

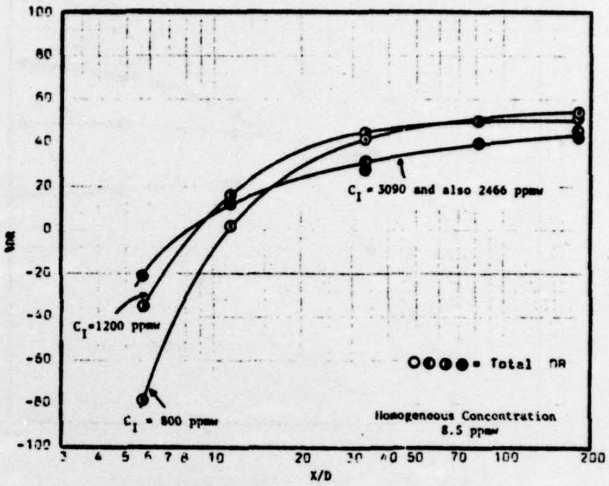

Fig. 3.11 Total drag reduction vs. X/D (C_∞ = 8.5 ppmw)

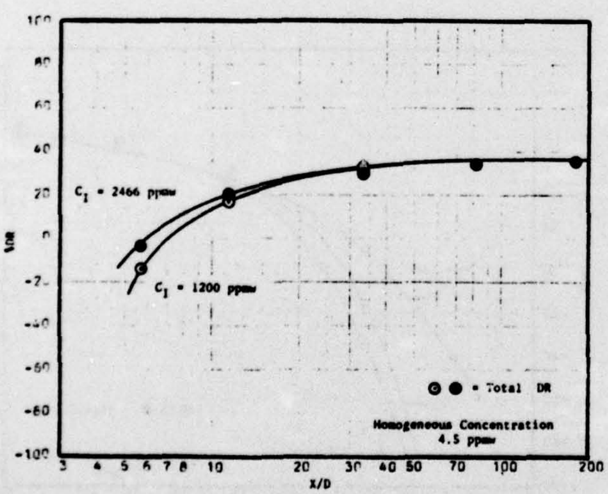

Fig. 3.12 Total drag reduction vs. X/D (C_∞ = 4.5 ppmw)

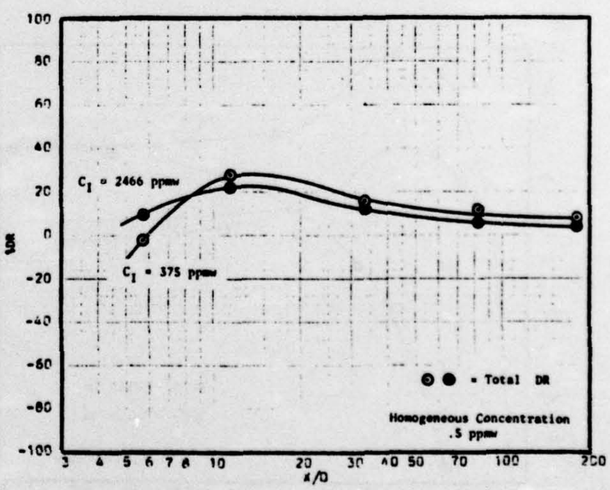

Fig. 3.13 Total drag reduction vs. X/D (C_∞ = .5 ppmw)

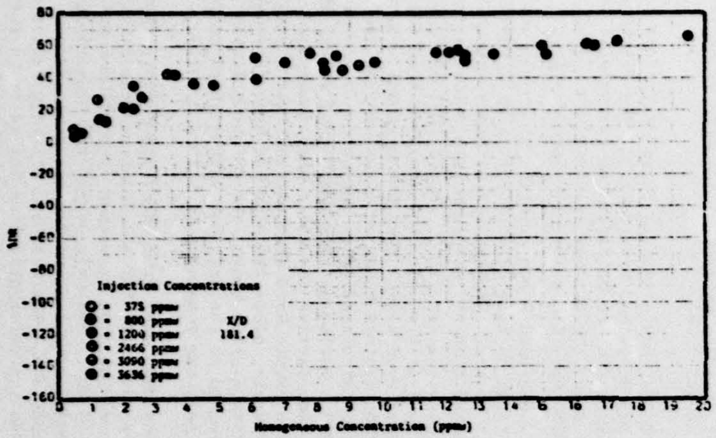

Fig. 3.14 Dependence of the total drag reduction on C_∞ (X/D = 181.4)

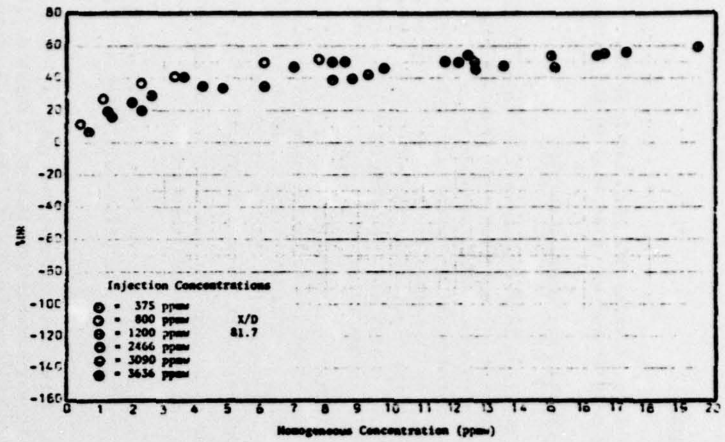

Fig. 3.15 Dependence of the total drag reduction on C_∞ (X/D = 81.7)

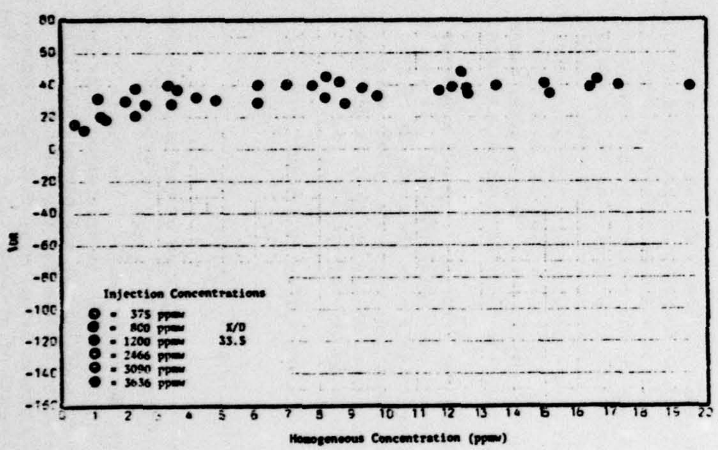

Fig. 3.16 Dependence of the total drag reduction on C_∞ (X/D = 33.5)

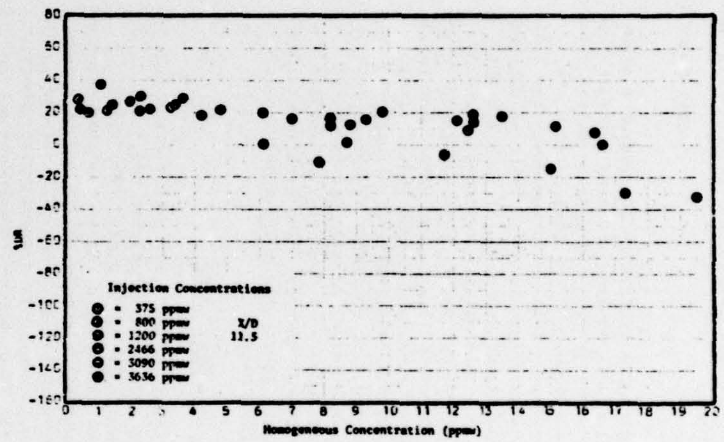

Fig. 3.17 Dependence of the total drag reduction on C_∞ (X/D = 11.5)

Chapter 4

DRAG REDUCTION WITH TRO-375

During the course of this investigation a study was made of the effect of drag-reducing additives on the cavitation of an orifice, as well as of the degradation of the polymers by the orifice flow (9). The degradation was determined by measuring the drag reduction of the solutions in a 1 5/8-in. galvanized pipe with an equivalent roughness of $\bar{K}/D = 0.00175$. The measurements of the friction factors of WSR 301, poly(ethylene oxide), solutions followed the friction factor curves corresponding to that particular roughness. Subsequent tests with Calgon TRO-375 (polyacrylamide) solutions consistently indicated, however, that the effective roughness of the pipe increased when this latter polymer was used. No direct visual evidence of a rougher pipe surface could be established, however. The experiments and the analysis which led to the above conclusion are described in this chapter.

Drag Reduction in a Rough Pipe

Previous studies (10,11,12) have already indicated that drag reduction by polymer additives is drastically reduced in rough pipes. The effect of the roughness is primarily a function of the relative size of the roughness elements $\bar{K}$ to the thickness of the viscous sublayer δ. When $\bar{K}/\delta$ is small, the pipe may be considered to be hydraulically smooth. When $\bar{K} \gg \delta$ the flow becomes independent of the viscosity of the fluid, and at the same time drag reduction disappears.

A simple semi-empirical model which attempts to describe the gross features of the effect of roughness on drag reduction has been offered by Poreh (10). The model is based on the assumption that the diminishing drag reduction is proportional to the diminishing role of the viscosity at large values of $\bar{K}/\delta$. (This role has been expressed by a function $P(\bar{K}/\delta)$). The function P was slightly modified in a later work following the discussion of the original paper (13). In this work the modified function was used.

To calculate the friction factor of a polymer solution in a rough pipe using the model, it is usually required to determine the behavior of the solution in a smooth pipe using the models which assume that the effect of the polymers is described by an upward shift of the log profile (14)

$$u/V^* = A \log (yV^*/\nu) + B + \Delta u^+$$

where

$$\Delta u^+ = \alpha \log (V^*/V^*_{crit}) \ .$$

The parameter α is a function of the concentration, whereas the critical shear V^*_{crit} is primarily a function of the molecular weight. The equivalent roughness of the pipe $\bar{K}/D$ is determined using pure water. No other coefficients are needed, but it is usually required to account for the existence of non-uniform roughness by assuming that the roughness is made of elements of at least two sizes: $K_1 = \bar{K}/Z$ and $K_2 = \bar{K}\cdot Z$. A value of $Z=2$ had been found to give good results and was also used in this study.

Analysis of the Experimental Results

The friction factors measured in flows of fresh and degraded WSR 301 solutions are shown in Fig. 4.1. The figure also shows calculated friction factor curves using the model of Poreh. One sees from this figure that the experimental data can be fairly well described by the model using the relative roughness, $\bar{K}/D = 0.00175$, which had been determined in water flows, and a common value of V^*_{crit} for all the fresh solutions. The behavior of the degraded 15 ppm solution can be described by the same value of α used for the 15 ppm fresh solution, which is consistent with the assumption that α is a function of the concentration, but here a different V^*_{crit} had to be used to account for the decrease of the molecular weight of the degraded solution.

The measurements of the friction factors in flows of fresh TRO-375 solutions are shown in Fig. 4.2.

None of the calculated curves with $\bar{K}/D = 0.00175$ appeared to satisfactorily match the measured data. The observed minimum in the f versus Re number curve shifted to lower Reynolds numbers and this change could be described with the model by increasing the effective roughness of the pipe up to values of $\bar{K}/D$ around 0.003.

The measurements using a degraded TRO-375 10 ppm solution are described in Fig. 4.3. The friction factor curves seem to be described fairly well by the model using the earlier values of $\alpha = 15.5$ and $K/D = 0.003$, but with a larger value of V^*_{crit}. Finally, a degraded 2 ppm solution which had been passed through an orifice at a very high Reynolds number was tested. Previous experiments with WSR-301 suggested that the solution should lose all of its drag-reducing capacity. Indeed that had happened but, as shown in Fig. 4.3, the measured friction factors were even higher than the original values of the friction factors measured in water flow and matched the calculated curve for water in a pipe with $\bar{K}/D = 0.003$. Following this surprising result the pipe friction factors for water were remeasured. These measurements have also matched the $\bar{K}/D = 0.003$ curve. However, after the pipe had been thoroughly cleaned with a nylon brush, the friction factors for water returned to the original values which correspond to relative roughness of $\bar{K}/D = 0.00175$.

It was concluded from these experiments that during the work with TRO-375 solutions the effective roughness of the pipe increased from $\bar{K}/D = 0.00175$ to $\bar{K}/D = 0.003$. Analysis of earlier measurements with degraded solutions of TRO-375 revealed several more records where the measured friction factor was higher than the original values for water in the cleaned pipe. It was not clear whether this

phenomenon was caused by slow accumulation of dirt or by an inherent property of this polymer. In an attempt to answer this question the pipe was cleaned and the friction factor for fresh 2 ppm solution of TRO-375 at a constant Reynolds number was recorded as a function of time. The data are plotted in Fig. 4.4 and they clearly show a rapid increase of the friction factor with time which supports the previous conclusion that a buildup of roughness is caused by the polymer. The variation is not due to degradation of the polymer since it was not recirculated.

It has also been observed that the roughness buildup in flows of fresh TRO-375 solutions did not wash out readily in water, but highly degraded solutions of this polymer did not produce a similar roughness increase.

Constraints imposed on this investigation made it impossible to conduct a more comprehensive study of this phenomena and determine if its effect is large enough to be of engineering significance. It is highly recommended that this apparent roughness buildup be further investigated.

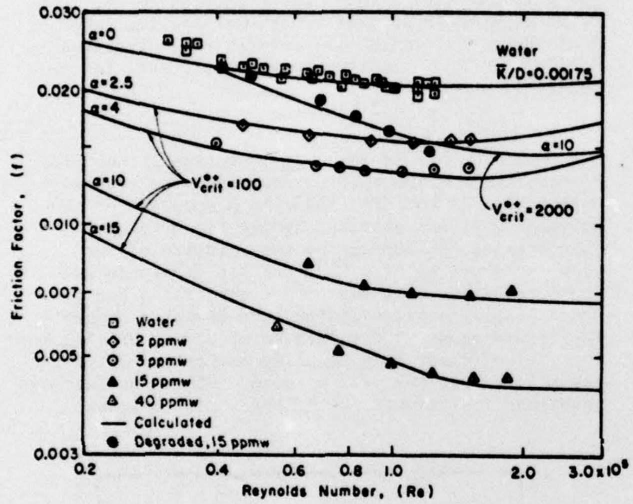

Fig. 4.1 Friction factors for WSR-301 solutions

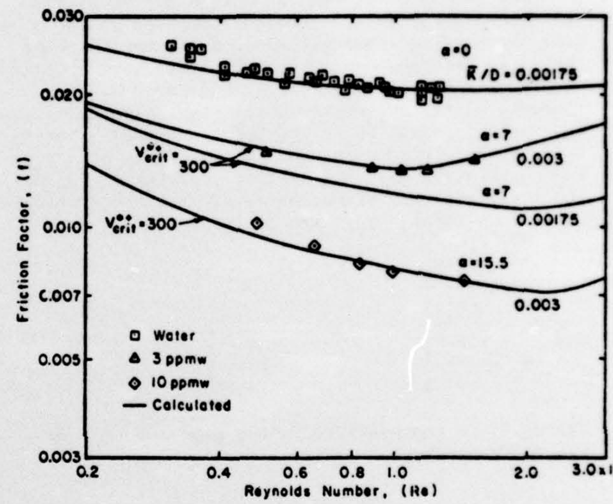

Fig. 4.2 Friction factors for fresh TRO-375 solutions

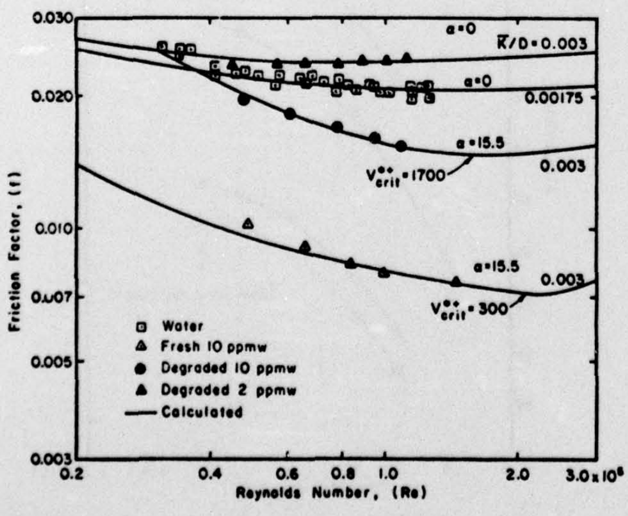

Fig. 4.3 Friction factors for TRO-375 solutions

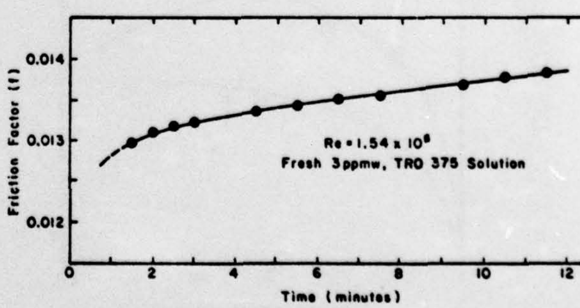

Fig. 4.4 Change of the friction factor with time after cleaning the pipe

Chapter 5

SUPPRESSION OF ORIFICE CAVITATION BY POLYMER ADDITIVES

During the course of the project, a study of the effect of drag reducing polymer on the cavitation of a 1/8-inch thick, square-edge orifice with a 0.62-inch diameter in a 1 5/8-inch pipe was conducted. The results are of interest to those working with polymer solutions and are therefore summarized below. The full investigation is described in Ref. (9).

The intensity of the cavitation at the orifice was monitored by an accelerometer mounted on the pipe near the orifice. The plotting of the rms value of the noise recorded by the accelerometer versus the square of the velocity, clearly indicated a sharp increase of the noise at a particular velocity, V_i, and a second break in the curve at a higher velocity, V_c. These points correspond to the points of incipient cavitation (i), and critical cavitation (C) (9). The incipient cavitation index, σ_i, and the critical cavitation index, σ_c, are defined as:

$$\sigma_i = \frac{P-P_v}{\rho V_i^2/2}$$

and

$$\sigma_c = \frac{P-P_v}{\rho V_c^2/2}$$

where P *is the pressure in the pipe and* P_v is the vapor pressure.

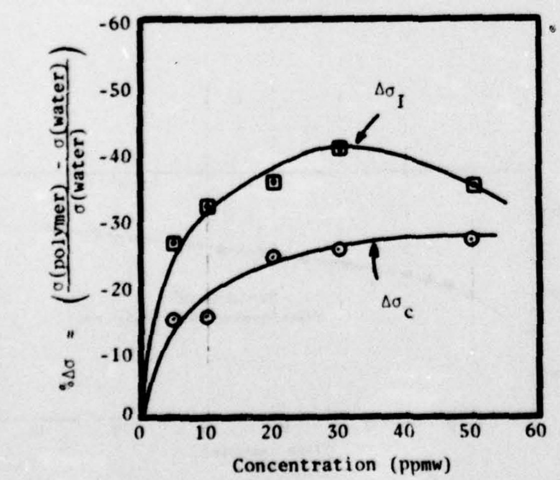

Fig. 5.1 Effect of polymer additives (WSR-301) on incipient and critical cavitation

The effect of polymer on σ_i and σ_c is shown in Fig. 5.1. A clear reduction of both σ_i and σ_c, due to the additives, is evident. This indicates that the addition of the polymers enables one to increase the velocities in the pipe before cavitation occurs, or to suppress the intensity of the cavitation at a given velocity. The effect of the polymers is larger on the incipient cavitation than on the critical cavitation. The reduction in σ_i can be as high as 40 percent. One must realize, however, that the corresponding increase in the velocities is smaller since σ is inversely proportional to the square of the velocity.

Measurements of the drag reduction in the pipe downstream from the orifice have revealed severe degradation of the drag reducing properties of the polymer solutions passing through the orifice. This degradation depends on the velocity of the flow, as shown in Fig. 5.2, but its magnitude was found to be the same for both a cavitating and a noncavitating orifice at the same Reynolds number. The figure shows that dilute solutions of WSR-301 have lost all of their drag reducing properties after passing through the orifice once. Other concentrated solutions lost around 50% of their effectiveness.

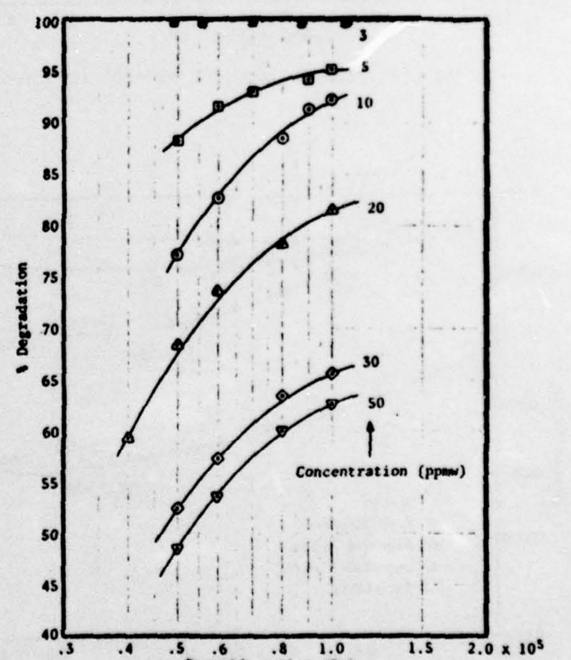

Fig. 5.2 Percent degradation versus Reynolds number for one pass through the orifice (WSR-301)

REFERENCES

1. Tullis, J. P. and L. F. Lindeman, Polymer injection for drag reduction. Naval Ship Research and Development Center Report, July 1972.

2. Tullis, J. P. and K. L. V. Ramu, Viscous drag reduction in developing pipe flow. Hydro Machinery Laboratory Report No. 34, Nov. 1973.

3. Wang, J. S. and J. P. Tullis, Turbulent flow in the entry region of a rough pipe. Journal of Fluid Engineering, ASME, Nov. 1973, (Paper No. 73-WA/FE-3).

4. Tullis, J. P. and K. L. V. Ramu, Drag reduction in developing pipe flow with polymer injection. International Conference on Drag Reduction, Cambridge, England, Sept. 1974, (Paper G3).

5. Ramu, K. L. V., Inlet region flow with polymer additives. Ph.D. Dissertation, Colorado State University, 1975.

6. Poreh, M., H. Rubin, and C. Plata, Studies in rheology and hydrodynamics of dilute polymer solutions. Pub. No. 126, Dept. Civ. Eng., Technion IIT, Haifa, Israel, 1969.

7. Poreh, M. and Y. Dimant, Velocity distribution and friction factors in pipe flows with drag reduction. Proc. Int. Sym. Naval Hydrodynamics (9th), Vol. 2, pp. 1305-1323, 1972, (AD-A010-506).

8. Walters, R. R. and C. S. Wells, Effect of distributed injection of polymer solution on turbulent diffusion. J. Hydronautics, 6, No. 2, pp. 69-76, 1972.

9. Hooper, John A., Pipe orifice flow with polymer additives. M.S. Thesis, Colorado State University, 1976.

10. Poreh, M., Flow of polymer solutions in rough pipes. J. Hydronautics, 4, 1, pp. 151-155, 1970.

11. Virk, P. S., Drag reduction in rough pipes. J. Fluid Mech., 12, p. 522, 1968.

12. Spangler, J. G., Studies of viscous drag reduction with polymers including turbulence measurements and roughness effects. In "Viscous Drag Reduction," pp. 131-157, C. S. Wells, ed., Plenum Press, N.Y., 1969.

13. Fabula, A. G. and D. M. Nelson, Comments on flow of dilute polymer solutions in rough pipes. Technical Comments, and Author's Reply, J. of Hydronautics, 5, No. 4, 1971.

14. Meyer, W. A., A correlation of the frictional characteristics for turbulent flow of dilute non-Newtonian fluids in pipes. A.I.Ch.E. J., 12, pp. 522-525, 1966.

DISTRIBUTION LIST FOR REPORTS PREPARED UNDER THE
GENERAL HYDROMECHANICS RESEARCH PROGRAM

40 Commander
David W. Taylor Naval Ship
Research and Development Center
Bethesda, Md 20084
Attn: Code 1505 (1)
Code 5211.4 (39)

1 Officer-in-Charge
Annapolis Laboratory
Naval Ship Research and
Development Center
Annapolis, Maryland 21402
Attn: Code 522.3 (Library)

7 Commander
Naval Sea Systems Command
Washington, D. C. 20360
Attn: SEA 09G32 (3 cys)
SEA 03512 (Peirce)
SEA 037
SEA 0322
SEA 033

12* Director
Defense Documentation Center
5010 Duke Street
Alexandria, Virginia 22314

1 Office of Naval Research
800 N. Quincy Street
Arlington, Virginia 22217
Attn: Mr. R. D. Cooper (Code 438)

1 Office of Naval Research
Branch Office
492 Summer Street
Boston, Mass 02210

1 Office of Naval Research
Branch Office (493)
536 S. Clark Street
Chicago, Illinois 60605

1 Chief Scientist
Office of Naval Research
Branch Office
1030 E. Green Street
Pasadena, CA 91106

1 Office of Naval Research
Resident Representative
715 Broadway (5th Floor)
New York, New York 10003

1 Office of Naval Research
San Francisco Area Office
760 Market St., Rm 447
San Francisco, CA 94102

2 Director
Naval Research Laboratory
Washington, D. C. 20390
Attn: Code 2027
Code 2629(ONRL)

1 Commander
Naval Facilities Engineering
Command(Code 032C)
Washington, D. C. 20390

1 Library of Congress
Science & Technology Division
Washington, D. C. 20540

1 Commander
Naval Electronics Laboratory
Center (Library)
San Diego, CA 92152

8 Commander
Naval Ship Engineering Center
Center Building
Prince Georges Center
Hyattsville, Maryland 20782
Attn: SEC 6034B
SEC 6110
SEC 6114H
SEC 6120
SEC 6136
SEC 6144G
SEC 6140B
SEC 6148

1 Naval Ship Engineering Center
Norfolk Division
Small Craft Engr Dept
Norfolk, Virginia 23511
Attn: D. Blount (6660.03)

1 Library (Code 1640)
Naval Oceanographic Office
Washington, D. C. 20390

1 Technical Library
Naval Proving Ground
Dehlgren, Virginia 22448

1 Commander (ADL)
Naval Air Development Center
Warminster, PA 18974

1 Naval Underwater Weapons Research
& Engineering Station (Library)
Newport, R.I. 02840

1 Commanding Officer (L31)
Naval Civil Engineering Laboratory
Port Hueneme, CA 93043

4 Commander
Naval Undersea Center
San Diego, CA 92132
Attn: Dr. A. Fabula (6005)
Dr. J. Hoyt (2501)
Library (13111)

1 Director
Naval Research Laboratory
Underwater Sound Reference Division
P.O. Box 8337
Orlando, Florida 32806

1 Library
Naval Underwater Systems Center
Newport, R. I. 02840

1 Research Center Library
Waterways Experiment Station
Corp of Engineers
P.O. Box 631
Vicksburg, Mississippi 39180

2 National Bureau of Standards
Washington, D. C. 20234
Attn: P. Kelbanoff (FM 105)
Fluid Mechanics
Hydraulic Section

1 AFOSR/NAM
1400 Wilson Blvd.
Arlington, Virginia 22209

1 AFFOL/FYS (J. Olsen)
Wright Patterson AFB
Dayton, Ohio 45433

1 Dept. of Transportation
Library TAD-491.1
400 - 7th Street S.W.
Washington, D. C. 20590

1 Charleston Naval Shipyard
Technical Library
Naval Base
Charleston, S. C. 29408

1 Norfolk Naval Shipyard
Technical Library
Portsmouth, Virginia 23709

1 Philadelphia Naval Shipyard
Philadelphia, PA 19112
Attn: Code 240

1 Portsmouth Naval Shipyard
Technical Library
Portsmouth, N. H. 03801

1 Puget Sound Naval Shipyard
Engineering Library
Bremerton, Wash. 98314

1 Long Beach Naval Shipyard
Technical Library (246L)
Long Beach, CA 90801

1 Hunters Point Naval Shipyard
Technical Library (Code 202.3)
San Francisco, CA 94135

1 Pearl Harbor Naval Shipyard
Code 202.32
Box 400, FPO
San Francisco, CA 96610

1 Mare Island Naval Shipyard
Shipyard Technical Library
Code 202.3
Vallejo, CA 94592

1 Assistant Chief Design Engineer
for Naval Architecture (Code 250)
Mare Island Naval Shipyard
Vallejo, CA 94592

3 U. S. Naval Academy
Annapolis, Maryland 21402
Attn: Technical Library
Dr. Bruce Johnson
Prof. P. Van Mater, Jr.

3 Naval Postgraduate School
Monterey, CA 93940
Attn: Library, Code 2124
Dr. T. Sarpkaya
Prof. J. Miller

1 Capt. L. S. McCready, USMS
Director, National Maritime
Research Center
U.S. Merchant Marine Academy
Kings Point, L.I., N.Y. 11204

1 U. S. Merchant Marine Academy
Kings Point, L.I., N.Y. 11204
Attn: Academy Library

1 Library
The Pennsylvania State University
Ordnance Research Laboratory
P.O. Box 30
State College, PA 16801

1 Bolt, Beranek & Newman
1701 N. For Myer Drive
Arlington, Virginia 22211
Attn: Dr. F. Jackson

1 Bolt, Beranek & Newman
50 Moulton Street
Cambridge, Mass. 02138
Attn: Library

1 Bethlehem Steel Corporation
Center Technical Division
Sparrows Point Yard
Sparrows Point, Maryland 21219

1 Bethlehem Steel Corporation
25 Broadway
New York, New York 10004
Attn: Library (Shipbuilding)

1 Cambridge Acoustical Associates, Inc.
1033 Mass Avenue
Cambridge, Mass 02138
Attn: Dr. M. Junger

1 CALSPAN Corporation
P.O. Box 235
Buffalo, New York 14221
Attn: Dr. A. Ritter
Aerodynamics Res. Dept.

1 Esso International
Design Division, Tanker Dept.
15 West 51st Street
New York, New York 10019

1 Mr. V. Boatwright, Jr.
R & D Manager
Electric Boat Division
General Dynamics Corporation
Groton, Conn 06340

1 Gibbs & Cox, Inc.
21 West Street
New York, New York 10006
Attn: Technical Info. Control

1 Hydronautics, Inc.
Pindell School Road
Howard County
Laurel, Maryland 20810
Attn: Library

2 McDonnell Douglas Aircraft Co.
3855 Lakewood Blvd
Long Beach, CA 90801
Attn: J. Hess
T. Cebeci

1 Lockheed Missiles & Space Co.
P.O. Box 504
Sunnyvale, CA 94088
Attn: Mr. R. L. Waid, Dept 57-74
Bldg. 150, Facility 1

1 Newport News Shipbuilding &
Dry Dock Company
4101 Washington Avenue
Newport News, Virginia 23607
Attn: Technical Library Dept.

1 North American Aviation, Inc.
Space & Information Systems Div.
12214 Lakewood Blvd.
Downey, CA 90241
Attn: Mr. Ben Ujihara (SL-20)

1 Nielsen Engineering & Research Inc.
510 Clyde Avenue
Mountain View, CA 94043
Attn: Mr. S. Spangler

1 Oceanics, Inc.
Technical Industrial Park
Plainview, L.I., N.Y. 11803

1 Society of Naval Architects
and Marine Engineers
74 Trinity Place
New York, New York 10006
Attn: Technical Library

1 Sperry Systems Management Division
Sperry Rand Corporation
Great Neck, N. Y. 11020
Attn: Technical Library

1 Stanford Research Institute
Menlo Park, CA 94025
Attn: Library G-021

1 Southwest Research Institute
P. O. Drawer 28510
San Antonio, Texas 78284
Attn: Applied Mechanics Review
Dr. H. Abramson

1 Tracor, Inc.
6500 Tracor Lane
Austin, Texas 78721

1 Mr. Robert Taggart
3930 Walnut Street
Fairfax, Virginia 22030

1 Ocean Engr Department
Woods Hole Oceanographic Inst.
Woods Hole, Mass. 02543

1 Worcester Polytechnic Inst.
Alden Research Laboratories
Worcester, Mass. 01609
Attn: Technical Library

1 Applied Physics Laboratory
University of Washington
1013 N.E. 40th Street
Seattle, Washington 98105
Attn: Technical Library

1 University of Bridgeport
Bridgeport, Conn. 06602
Attn: Dr. E. Uram

1 Cornell University
Graduate School of Aerospace Engr
Ithaca, New York 14850
Attn: Prof. W. R. Sears

4 University of California
Naval Architecture Department
College of Engineering
Berkeley, CA 94720
Attn: Library
Prof. W. Webster
Prof. J. Paulling
Prof. J. Wehausen

3 California Institute of Technology
Pasadena, CA 91109
Attn: Aeronautics Library
Dr. T. Y. Wu
Dr. A. J. Acosta

1 Docs/Repts/Trans Section
Scripps Institution of
Oceanography Library
University of California, San Diego
P.O. Box 2367
La Jolla, CA 92037

1 Catholic University of America
Washington, D. C. 20017
Attn: Dr. S. Heller, Dept of
Civil & Mech Engr

1 Colorado State University
Foothills Campus
Fort Collins, Colorado 80523
Attn: Branch Library, Engr Res Center

1 University of California at San Diego
La Jolla, CA 92038
Attn: Dr. A. T. Ellis
Dept. of Applied Math

2 Florida Atlantic University
Ocean Engineering Department
Boca Raton, Fla 33432
Attn: Technical Library
Dr. S. Dunne

2 Harvard University
Pierce Hall
Cambridge, Mass. 02138
Attn: Prof. G. Carrier
Gordon McKay Library

1 University of Hawaii
Department of Ocean Engineering
2565 The Mall
Honolulu, Hawaii 96822
Attn: Dr. C. Bretschneider

1 University of Illinois
Urbana, Illinois 61801
Attn: Dr. J. Robertson

3 Institute of Hydraulic Research
The University of Iowa
Iowa City, Iowa 52240
Attn: Library
Dr. L. Landweber
Dr. J. Kennedy

1 The John Hopkins University
Baltimore, Md 21218
Attn: Prof. O. Phillips
Mechanics Dept

1 Kansas State University
Engineering Experiment Station
Seaton Hall
Manhattan, Kansas 66502
Attn: Prof. D. Nesmith

1 University of Kansas
Chm Civil Engr Dept Library
Lawrence, Kansas 60644

5 Department of Ocean Engineering
Massachusetts Institute of Technology
Cambridge, Mass 02139
Attn: Department Library
Prof. P. Leehey
Prof. P. Mandel
Prof. M. Abkowitz
Dr. J. Newman

1 Parsons Laboratory
Massachusetts Institute of Technology
Cambridge, Mass 02139
Attn: Prof. A. Ippen

5 St. Anthony Falls Hydraulic Laboratory
University of Minnesota
Mississippi River at 3rd Avenue S.E.
Minneapolis, Minnesota 55414
Attn: Prof. E. Silberman
Mr. J. Wetzel
Mr. F. Schiebe
Mr. J. Killen
Dr. C. Song

3 Department of Naval Architecture and Marine Engineering
University of Michigan
Ann Arbor, Michigan 48104
Attn: Library
Dr. T. F. Ogilvie
Prof. F. Hammitt

2 College of Engineering
University of Notre Dame
Notre Dame, Indiana 46556
Attn: Engineering Library
Dr. A. Strandhagen

2 New York University
Courant Inst. of Math. Sciences
251 Mercier Street
New York, New York 10012
Attn: Prof. A. Peters
Prof. J. Stoker

1 New York University
University Heights
Bronx, New York 10453
Attn: Prof. W. Pierson, Jr.

1 Department of Aerospace & Mechanical Sciences
Princeton University
Princeton, N. J. 08540
Attn: Prof. G. Mellor

3 Davidson Laboratory
Stevens Institute of Technology
711 Hudson Street
Hoboken, New Jersey 07030
Attn: Library
Mr. J. Breslin
Mr. S. Tsakonas

1 Applied Research Laboratory Library
University of Texas
P.O. Box 8029
Austin, Texas 78712

1 College of Engineering
Utah State University
Logan, Utah 84321
Attn: Dr. R. Jeppson

2 Stanford University
Stanford, CA 94305
Attn: Engineering Library
Dr. R. Street

3 Webb Institute of Naval Architecture
Crescent Beach Road
Glen Cover, L.I., N.Y. 11542
Attn: Library
Prof. E. V. Lewis
Prof. L. W. Ward

1 National Science Foundation
Engineering Division Library
1800 G Street N. W.
Washington, D. C. 20550

1 University of Connecticut
Box U-37
Storrs, Conn 06268
Attn: Dr. V. Scottron
Hydraulic Research Lab

1 Applied Research Laboratory
P.O. Box 30
State College, Pa 16801
Attn: Dr. B. Parkin, Director
Garfield Thomas Water Tunnel

1 Dr. Michael E. McCormick
Naval Systems Engineering Department
U. S. Naval Academy
Annapolis, Maryland 21402

1 Dr. Douglas E. Humphreys (Code 712)
Naval Coastal Systems Laboratory
Panama City, Florida 32401

UNCLASSIFIED

SECURITY CLASSIFICATION OF THIS PAGE (When Data Entered)

REPORT DOCUMENTATION PAGE | **READ INSTRUCTIONS BEFORE COMPLETING FORM**

1. REPORT NUMBER
2. GOVT ACCESSION NO.
3. RECIPIENT'S CATALOG NUMBER

9

4. TITLE (and Subtitle)

6 POLYMER INJECTION INTO A DEVELOPING BOUNDARY LAYER

5. TYPE OF REPORT & PERIOD COVERED

Final Report, 1 Oct 74 - 31 Mar 76

10/1/74 to 3/31/76

6. PERFORMING ORG. REPORT NUMBER

14 HM-71

7. AUTHOR(s)

10 J. Paul Tullis, Michael Poreh and John A. Hooper

8. CONTRACT OR GRANT NUMBER(s)

N00014-75-C-0274 new

15

9. PERFORMING ORGANIZATION NAME AND ADDRESS

Engineering Research Center
Colorado State University
Fort Collins, Colorado 80521

10. PROGRAM ELEMENT, PROJECT, TASK AREA & WORK UNIT NUMBERS

16

61153N R023 01

17 SR 023 01 01

11. CONTROLLING OFFICE NAME AND ADDRESS

David W. Taylor Naval Ship Research and
Development Center (Code 1505)
Bethesda, Maryland 20084

12. REPORT DATE

11 March 1976

13. NUMBER OF PAGES

26 12 24p.

14. MONITORING AGENCY NAME & ADDRESS(if different from Controlling Office)

Office of Naval Research
800 N. Quincy St
Arlington, Virginia 22217

15. SECURITY CLASS. (of this report)

Unclassified

15a. DECLASSIFICATION/DOWNGRADING SCHEDULE N/A

16. DISTRIBUTION STATEMENT (of this Report)

APPROVED FOR PUBLIC RELEASE: DISTRIBUTION UNLIMITED

17. DISTRIBUTION STATEMENT (of the abstract entered in Block 20, if different from Report)

N/A

18. SUPPLEMENTARY NOTES

Sponsored by the Naval Sea Systems Command, General Hydromechanics Research (GHR) Program administered by the David W. Taylor Naval Ship Research and Development Center (Code 1505), Bethesda, Maryland 20084

19. KEY WORDS (Continue on reverse side if necessary and identify by block number)

GHR Program, Polymers, Polymer injection, Polymer degradation, Drag reduction, Cavitation suppression, Cavitating orifice, Boundary layer

20. ABSTRACT (Continue on reverse side if necessary and identify by block number)

This report describes the last phase of a study on the drag reduction at the entrance region of a 12-inch pipe by injection of polymer solutions. In this phase of the study the effect of injecting concentrated solutions of WSR 301, up to 3600 ppmw, was examined.

This study indicates that the local friction downstream from the injector can be considerably reduced by increasing the discharge of the polymer

next page

DD FORM 1473, 1 JAN 73 EDITION OF 1 NOV 65 IS OBSOLETE
S/N 0102-LF-014-6601

UNCLASSIFIED 408 396

SECURITY CLASSIFICATION OF THIS PAGE (When Data Entered)

bpg

20. Abstract - continued

cont

injected into the pipe. However, the injection disturbs the flow and increases the pressure losses across the injector.

When the total drag reduction of a given pipe length (X/D), which includes the losses due to the injection, is considered, it is found that different optimal conditions exist for reducing the drag of short pipe sections and for reducing the drag of long pipe sections.

This report also summarizes a study of drag reduction in a pipe flow of Calgon TRO-375 solutions. For certain tests, this polymer caused an apparent increase in the effective roughness of the pipe walls. In addition, the report summarizes a study of the effect of a polymer (WSR 301) on the cavitation characteristics of a pipe orifice.